How to cite: *Angew. Chem. Int. Ed.* **2025**, *64*, e202505639
doi.org/10.1002/anie.202505639

Photocatalysis

Mixed-Metal Ce-Zr-Mn Clusters as Photo-Catalysts for Decarboxylative Functionalization of Carboxylic Acids

*Sota Tamaki, Riina Kuwata, Shuto Wakita, Yasuko Osakada, Mamoru Fujitsuka, Tetsuro Kusamoto, Kazushi Mashima, and Hayato Tsurugi**

Abstract: Decarboxylative hydrazination of carboxylic acids was achieved using a 1:5:2 ratio of three metal salts, $Ce(O^tBu)_4$, $Zr(O^tBu)_4$, and $Mn(OAc)_3$, as a catalyst under visible light irradiation. The catalytic activity, compared with our previously developed Ce_6 cluster photo-catalysts, was enhanced by the formation of single cerium-incorporated hexanuclear mixed-metal clusters containing a $[CeZr_5O_4(OH)_4]^{12+}$ core. The manganese salts further accelerated the overall reaction rate (10 times faster reaction rate with the manganese salt than that of the manganese-free conditions). Using the isolated cluster, $CeZr_5O_4(OH)_4(OCOCH_2{}^tBu)_{12}(HOCOCH_2{}^tBu)_4$ (**4a**), with $Mn(OAc)_3$, phenol and thiophenol-containing carboxylic acids were transformed to their decarboxylative hydrazinated products in moderate to high yields, while a mixture of $Ce_6O_4(OH)_4(OCOCH_2{}^tBu)_{12}(HOCOCH_2{}^tBu)_4$ (**4c**) and $Mn(OAc)_3$ or $Ce(O^tBu)_4$, $Zr(O^tBu)_4$, and $Mn(OAc)_3$ yielded lower amounts of the products. These findings highlight the importance of incorporating cerium(IV) into the zirconium-based core to tolerate these easily oxidizable functional groups. Upon exposure of **4a** to blue LED light under an argon atmosphere, the $CeZr_5$ cluster produced 2,2,5,5-tetramethylhexane, a radical coupling product derived from the carboxylate ligand on **4a**, in half an equivalent per cluster, consistent with the photo-reduction of cerium(IV) and inertness of the oxo- and hydroxo-bridged Zr_5 motif as a metallo-ligand around the cerium(IV) site. Moreover, decarboxylative oxygenation of carboxylic acids under air followed by treatment with $NaBH_4$ resulted in the production of one-carbon shortened alcohols in excellent yields when using $Ce(O^tBu)_4$ and $Zr(O^tBu)_4$ or $Hf(O^tBu)_4$ in a 1:5 ratio: the reaction rates were 8–10 times higher than that of the previously developed cerium-catalyzed reaction under identical conditions.

The use of light energy in chemical reactions is an important strategy for promoting sustainable development. The utilization of light energy as a cleaner and renewable alternative to conventional energy sources derived from fossil fuels is extensively investigated. In the field of synthetic organic chemistry, the application of light energy offers a distinct advantage by selectively promoting desired reactions through the excitation of specific reactants, functional groups, and catalysts.[1–5] This method not only reduces energy loss but also prevents the degradation of unwanted functional groups, thus largely differing from thermal reactions requiring energy for both reactants and the surrounding media.

A prominent example of utilizing photo-energy in organic synthesis is the decarboxylation and functionalization of carboxylic acids under photo-irradiation, which provides a direct approach to convert readily available, stable, and naturally occurring carboxylic acids into various valuable organic compounds.[6–11] The key step in this process is the generation of carboxyl radicals by the photolysis of metal carboxylate complexes[12–16]: high oxidation state metal carboxylate complexes, such as cerium(IV),[17–32] iron(III),[33–58] and copper(II),[59–69] can be photo-excited to induce homolysis of the metal-carboxylate bond, leading to the formation of synthetically useful carboxyl radicals through ligand-to-metal charge transfer (LMCT). Carboxylic acids containing redox-labile substituents, however, such as phenols, thioanisoles, alcohols, and electron-rich aromatic rings, commonly found in natural carboxylic acid scaffolds, present challenges for decarboxylative transformations due to their limited compatibility with high-oxidation state metal complexes.[70,71]

[*] Dr. S. Tamaki, Prof. Dr. T. Kusamoto
Department of Chemistry, Graduate School of Engineering Science, The University of Osaka, Toyonaka, Osaka, Japan

R. Kuwata, S. Wakita, Prof. Dr. H. Tsurugi
Department of Applied Chemistry, Graduate School of Engineering, The University of Osaka, Suita, Osaka, Japan
E-mail: tsurugi@chem.eng.osaka-u.ac.jp

Dr. Y. Osakada, Prof. Dr. M. Fujitsuka
SANKEN (The Institute of Scientific and Industrial Research), The University of Osaka, Ibaraki, Japan

Dr. Y. Osakada, Prof. Dr. M. Fujitsuka, Prof. Dr. H. Tsurugi
Innovative Catalysis Science Division, Institute for Open and Transdisciplinary Research Initiatives (ICS-OTRI), The University of Osaka, Suita, Osaka, Japan

Prof. Dr. K. Mashima
Graduate School of Pharmaceutical Sciences, The University of Osaka, Suita, Osaka, Japan

Additional supporting information can be found online in the Supporting Information section

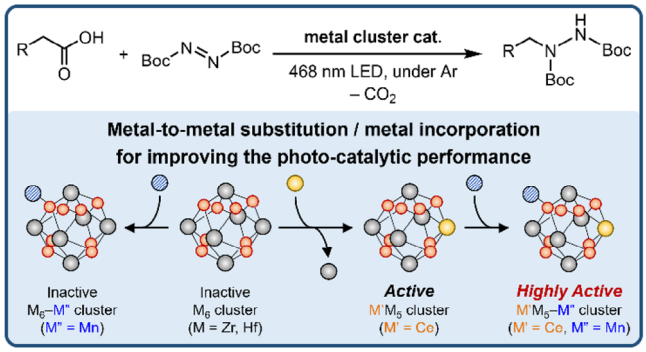

Figure 1. Modification of metal components in multi-metal cluster for decarboxylative functionalization of carboxylic acids.

In this context, cerium complexes have emerged as promising photo-catalysts for generating reactive radicals from carboxylic acids in organic synthesis. Our previous studies demonstrated that hexanuclear cerium(IV) clusters with oxo/hydroxo bridges and carboxylate ligands, $Ce_6O_4(OH)_4(OCOR)_{12}$, act as photo-catalysts for producing carboxyl radicals from carboxylic acids under blue LED irradiation, giving the decarboxylative oxygenated products, alcohols and carbonyl compounds, under a dioxygen atmosphere.[20] Based on this finding with cerium(IV) clusters, we herein report that incorporating a photo-responsive cerium(IV) center into photochemically robust oxo/hydroxo-bridged zirconium and hafnium clusters triggers higher catalytic activity for a decarboxylative hydrazination reaction compared with the corresponding homometallic clusters. In addition, adding a third component, typically manganese salts, to the cerium-containing cluster significantly enhanced the catalytic activity while low catalytic activity was observed for an original Zr_6 cluster combined with manganese salt, providing the first example of the three kinds of metals incorporated mixed-metal clusters as photo-catalysts in synthetic applications (Figure 1). Furthermore, these mixed-metal clusters exhibited remarkable efficiency in converting carboxylic acids containing phenol and thiophenol groups while preventing their oxidative degradation.

Catalyst Optimization

We began by searching for a highly active catalyst for the decarboxylative hydrazination of 4-fluorophenylacetic acid (**1a**) with an azo compound **2** under irradiation using 468 nm LED light (40 W) at room temperature in PhCl for 18 h (constant distance from the light to the test tube, 5 cm); the results are summarized in Table 1. Catalytic activity for the decarboxylative hydrazination was observed by combining $Ce(O^tBu)_4$ and $M(O^tBu)_4$ (M = Zr, Hf) in a 1:5 ratio, giving the hydrazinated product **3a** in moderate yields (entries 1 and 2). However, no product was obtained when using each component alone (entry 3, details in Table S1), suggesting that the in situ-formed heterometallic species was indispensable for the catalytic performance (vide infra). More importantly,

Table 1: Optimization of reaction conditions for decarboxylative hydrazination of **1a**.[a]

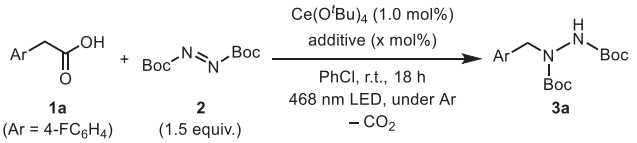

1a (Ar = 4-FC_6H_4) + **2** (1.5 equiv.) → **3a**

Entry	Additive (x mol%)	Yield [%][b]
1	$Zr(O^tBu)_4$ (5.0)	45
2	$Hf(O^tBu)_4$ (5.0)	22
3	–	n.d.
4	$Zr(O^tBu)_4$ (5.0), $Mn(OAc)_3{\cdot}2H_2O$ (2.0)	93 (85)[c]
5	$Hf(O^tBu)_4$ (5.0), $Mn(OAc)_3{\cdot}2H_2O$ (2.0)	86
6	$Zr(O^tBu)_4$ (5.0), $Mn(OAc)_2{\cdot}4H_2O$ (2.0)	78
7	$Zr(O^tBu)_4$ (5.0), $Fe(OAc)_2$ (2.0)	72
8	$Zr(O^tBu)_4$ (5.0), $Co(OAc)_2{\cdot}4H_2O$ (2.0)	70
9	$Zr(O^tBu)_4$ (5.0), $Ni(OAc)_2$ (2.0)	52
10	$Zr(O^tBu)_4$ (5.0), $Cu(OAc)_2$ (2.0)	76
11	$Zr(O^tBu)_4$ (5.0), $Zn(OAc)_2{\cdot}2H_2O$ (2.0)	40
12	$Mn(OAc)_3{\cdot}2H_2O$ (2.0)	49
13[d]	$Zr(O^tBu)_4$ (5.0), $Mn(OAc)_3{\cdot}2H_2O$ (2.0)	11
14	Cs_2CO_3 (2.0)	5
15	CsF (2.0)	21
16[e]	$Zr(O^tBu)_4$ (2.5), $Mn(OAc)_3{\cdot}2H_2O$ (1.0)	48

n.d., not detected. [a] Reaction conditions: **1a** (0.200 mmol), **2** (0.300 mmol), $Ce(O^tBu)_4$ (1.0 mol%), additive (x mol%), PhCl (3.0 mL), under Ar. Irradiated with 468 nm LED (distance between the light source and the test tube, 5 cm) [b] Determined by ^1H NMR using 1,3,5-trimethoxybenzene as an internal standard. [c] Isolated yield. [d] Without $Ce(O^tBu)_4$. [e] **1a** (0.400 mmol), **2** (0.600 mmol), and $Ce(O^tBu)_4$ (0.5 mol%).

adding a third component, 2.0 mol% of $Mn(OAc)_3{\cdot}2H_2O$, further improved the yield to afford **3a** in 93% yield with $Zr(O^tBu)_4$ (entry 4) and 86% yield with $Hf(O^tBu)_4$ (entry 5). A different of third component, such as $Mn(OAc)_2{\cdot}4H_2O$, $Fe(OAc)_2$, $Co(OAc)_2{\cdot}4H_2O$, and $Cu(OAc)_2$, also had positive effects on the decarboxylative hydrazination to afford **3a** (entries 6–8, 10), whereas $Ni(OAc)_2$ and $Zn(OAc)_2{\cdot}2H_2O$ were ineffective for improving the catalytic performance (entries 9 and 11). Among $M(acac)_3$ complexes of group 7–9 metals, $Mn(acac)_3$ also promoted the catalytic reaction to form **3a** in a high yield (Table S3, entry 7). On the other hand, a mixture of two components, $Ce(O^tBu)_4$ and $Mn(OAc)_3{\cdot}2H_2O$, showed moderate activity, and a mixture of $Zr(O^tBu)_4$ and $Mn(OAc)_3{\cdot}2H_2O$ exhibited much lower activity (entries 12 and 13). Previously, König et al. reported decarboxylative hydrazination by $CeCl_3$ combined with inorganic bases, but the catalytic activity of $Ce(O^tBu)_4$ with 1.0 mol% cerium catalyst loading for arylacetic acids was rather low under our reaction conditions in the presence of the inorganic salts (entries 14 and 15).[18] When the catalyst loading amounts were decreased to half of those used in the optimized reaction conditions, the yield of **3a** also decreased to nearly half (entry 16). Thus, the catalyst system of entry 4 (Ce, Zr, and Mn salts) was selected as the optimal catalyst system for further investigation of the substrate scope of carboxylic acids (vide infra).

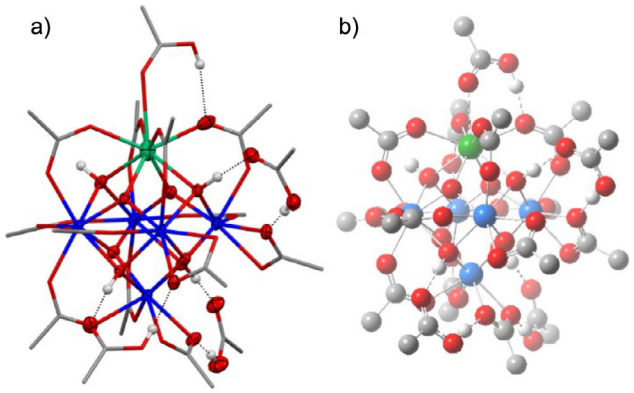

Figure 2. Molecular structure of **4a** determined by X-ray diffraction study (a, left) and DFT study (b, right). ^{t}Bu groups on the carboxylate ligands, and hydrogen atoms except for relating to the hydrogen bonding interaction are omitted for clarity. Green for cerium, blue for zirconium, red for oxygen, and gray for carbon atoms. Seven hydrogen bonding interactions are described as dot lines. a) Atoms in the $CeZr_5O_4(OH)_4$ core and carboxylate oxygen relating to the hydrogen bonding interaction with carboxylic acids are shown as thermal ellipsoids with 50% probability. Stick style is applied for other carboxylate moieties. Selected bond lengths (Å) of **4a**: Ce – O1 2.170(3), Ce – O2 2488(3), Ce – O3 2160 (3), Ce – O4 2.350(3), Zr1 – O10 2.206(3), Zr1 – O11 2.108(3), Zr1 – O12 2.212(3), Zr1 – O13 2.034(3).

Synthesis, Characterization, and Reactivity of Ce-Containing Clusters

Heterometallic clusters of $CeZr_5$ **4a** and $CeHf_5$ **4b** formed during the catalytic reaction were isolated by treating $Ce(O^tBu)_4$ and $M(OR)_4$ in an optimal 1:5 ratio under aerobic conditions in toluene with 3 equiv of *tert*-butylacetic acid relative to the total amounts of metal sources (Equation 1). In this reaction, substitution of one metal in the $[M_6O_4(OH)_4]^{12+}$ core with cerium(IV) gave the heterometallic core, $[CeM_5O_4(OH)_4]^{12+}$; in fact, treatment of $Zr_6O_4(OH)_4(OCOCH_2{}^tBu)_{12}$ with $Ce(O^tBu)_4$ in the presence of carboxylic acids produced corresponding heterometallic cluster **4a**. Cluster **4a** was isolated as a pale yellow microcrystalline solid in 74% yield, and the overall molecular structure was clarified by single crystal X-ray diffraction analysis (Figure 2a). Six metal ions, four oxo, and four hydroxo ligands form the central $[CeZr_5O_4(OH)_4]^{12+}$ core, which is surrounded by nine μ-η^1,η^1-carboxylate ligands, three η^2-carboxylate ligands on the three Zr atoms, and one *tert*-butylacetic acid on the cerium center through coordination of the oxygen atom of the carboxylate group. In addition, three *tert*-butylacetic acids locate around the $CeZr_5O_4(OH)_4$ core by hydrogen bonding with three bridging hydroxo ligands and η^2-carboxylate ligands. Due to the larger ionic radii of cerium than zirconium, the bond lengths of cerium and the bridging oxo and hydroxo ligands [2.160(3) Å and 2.171(3) Å for Ce – (μ_3-O); 2.350(3) Å and 2.488(3) Å for Ce – (μ_3-OH)] are longer than those around the Zr1 atom locating on the opposite side of the Ce [2.034(3) and 2.108(3) Å for Zr1 – (μ_3-O), 2.206(3) and 2.212(3) Å for Zr1 – (μ_3-OH)] (an enlarged ORTEP drawing and a table for the selected geometry in Figure S5 and Table S12). Noteworthy is that the cerium(IV) center possesses one neutrally coordinating carboxylic acid having a hydrogen bonding interaction with the adjacent μ-η^1,η^1-carboxylate ligands, which is clarified by DFT study of **4a** (vide infra). Homometallic Ce_6 and Zr_6 clusters surrounded by twelve carboxylate ligands are reported to date[28]; most of the clusters possess η^2- or μ-η^1,η^1-carboxylate ligation. The molecular structure of the hafnium variant **4b** is essentially the same as that of **4a** (Figures S5 and S6). The structurally similar cerium and zirconium heterometallic hexanuclear structures are reported for nodes of Ce and Zr-containing metal organic framework.[72–81]

The optimized structure of **4a** based on the DFT study, shown in Figure 2b, clarified the interesting features of the carboxylate ligand around the cerium center: a coordinating carboxylic acid on the cerium forms hydrogen bonding with the neighboring μ-η^1,η^1-carboxylate ligand, in which the length of the cerium and the oxygen bond of the μ-η^1,η^1-carboxylate ligand is 2.5139 Å, a value 0.08 – 0.15 Å longer than that of other cerium and oxygen bonds of μ-η^1,η^1-carboxylate ligands without the hydrogen bonding. We thus presume that deprotonation of the coordinating carboxylic acid by the adjacent bridging μ-η^1,η^1-carboxylate ligand on the cerium forms a η^1-carboxylate ligand prior to the carboxylate radical formation, which is the key factor for the facial carboxyl radical generation in this cerium-containing cluster (vide infra, Scheme 1). Generation of carboxylate radicals from the η^1-carboxylate ligand is faster than that from μ-η^1,η^1-carboxylate ligand, which likely relates to the higher catalytic performance of carboxylate clusters in the decarboxylative functionalization reactions.[62]

UV-Vis absorption spectra of **4a** and **4b** in toluene showed broad absorption in the range of UV-A to the blue light region (Figures S3 and S4), assignable to the LMCT, clearly indicating that a single cerium atom influences the HOMO-LUMO gap, thereby affecting photo-responsivity upon irradiation with a 468 nm LED light, though no absorption in the visible light region was observed for the corresponding Zr_6 cluster.[28] The LUMO to LUMO + 6 orbitals for **4a** clarified by DFT studies ascribe to the vacant 4f-orbitals of cerium in an energetically narrow range (0.134 eV, 0.00494 Hartree), and their energy levels are lower than the vacant 4d-orbitals of zirconium (HOMO to LUMO, 3.47 eV; HOMO to LUMO + 7, 5.90 eV) (Figures S19–S28). We also checked the TD-DFT analysis of **4a** to clarify the transition relating to the visible light region: the major transition in the visible light region originates from the lone pair of electrons of the carboxylate ligands and oxo/hydroxo bridging ligands to the vacant 4f-orbitals of cerium, suggesting LMCT as the key photo-responsivity for generating carboxylate radicals after visible light irradiation. No LMCT from the carboxylic acid on the cerium is found in the TD-DFT study, suggesting

the importance of the deprotonation to form η^1-carboxylate ligation for the LMCT process.

We further checked the reactivity of cluster **4a** under blue LED irradiation.[82] The formation of 2,2,5,5-tetramethylhexane was observed in half an equivalent to **4a** (Equation 2), whereas the same treatment for homometallic cerium cluster $Ce_6O_4(OH)_4(OCOCH_2{}^tBu)_{12}(OCOCH_2{}^tBu)_4$ (**4c**) produced three equivalents of 2,2,5,5-tetramethylhexane and insoluble cerium(III) precipitates due to the reduction of all the cerium(IV) centers to cerium(III).[20] One cerium(IV)-(η^1-carboxylate) bond for **4a**, formed after the deprotonation as mentioned above, selectively underwent homolysis without photo-reduction of the zirconium(IV) center, consistent with the large energy gap between the occupied orbitals relating to the oxo, hydroxo, and carboxylate ligands and vacant 4d-orbitals of the zirconium(IV) center (vide supra), though characterization of the photo-reduced cerium(III)-containing species was unsuccessful.

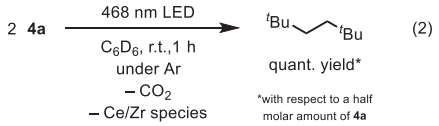

Based on the findings for cerium-containing hexanuclear clusters from two metal *tert*-butoxide complexes and carboxylic acids, we assumed that the additive effect of manganese salts in Table 1 is due to coordination of the bridging oxo ligand to the manganese to form trimetallic clusters, as observed for first-row transition metal-decorated oxo-bridged Zr_6 clusters containing a structurally similar $[Zr_6O_4(OH)_4]^{12+}$ core[83–87]; however, characterization of the mixed-metal clusters of cerium, zirconium, and manganese was unsuccessful. Aiming to clarify the oxidation state of the manganese species during the catalytic reaction, a solution of manganese(III) complexes was irradiated with visible light: their absorption in the visible light region was decreased to give a pale-colored solution assignable to the manganese(II) species (Figure S7), indicating that the manganese(II) species are present during the reaction and incorporated into **4a**. Thus, the role of manganese salts is assumed to increase the electron density within the mixed metal cluster, resulted in promoting reduction of the in situ-generated hydrazyl radical to form its anion and Ce(IV) center (vide infra, Scheme 1). In fact, Christou et al. reported that a combination of cerium and manganese served as an effective oxidation catalyst for alcohols under a dioxygen atmosphere due to the synergistic effect of the redox-active cerium and manganese.[88–92]

To clarify the influence of the manganese salt on the catalytic performance, the concentration of product **3b** under 390 nm LED irradiation was monitored for several catalyst combinations, as shown in Figure 3, in which $Mn(acac)_3$ was used as the manganese additive due to its better solubility in PhCl compared with $Mn(OAc)_3{\cdot}2H_2O$ and rapid photo-reduction in the presence of excess amounts of carboxylic acids via homolysis of the manganese-ligand covalent bond. $Mn(acac)_3$ significantly improved the reaction rate (k_{obs}) in this decarboxylative hydrazination reaction. The observed reaction rate by $CeZr_5$ cluster **4a** (1.0 mol%) and $Mn(acac)_3$ (2.0 mol%) was approximately 10 times faster than that

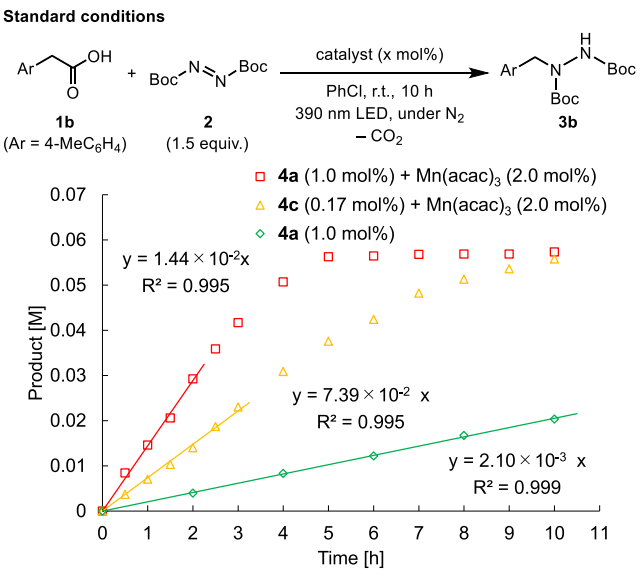

Figure 3. Time profiles for the formation of **3b**.

without $Mn(acac)_3$ (red vs. green lines). In addition, the catalytic reaction by Ce_6 cluster **4c** (0.17 mol%, 1.0 mol% on Ce) and $Mn(acac)_3$ (2.0 mol%) was slower than that induced by **4a**/$Mn(acac)_3$. Thus, we concluded that the combination of **4a** and the manganese complex generated the most active clusters in this decarboxylative hydrazination reaction. We also carried out a kinetic analysis; however, due to the strong absorption of **2** in the visible light region compared with the metal components, clarification of the reaction order of each component was unsuccessful (details in Figures S9–S16).

Reaction Mechanism for Decarboxylative Hydrazination Catalyzed by 4a and Manganese Salt

Based on the hydrogen bonding interaction found in the DFT study of **4a** as well as the reaction rate enhancement by the manganese additive, a possible reaction mechanism is shown in Scheme 1. Initially, one carboxylic acid coordinates to the cerium(IV) center to form **A** having a hydrogen bonding interaction with the proximal carboxylate ligand, as proposed by the structurally characterized $CeZr_5$ cluster **4a** and the DFT study. Subsequently, proton on the coordinating carboxylic acid transfers to form η^1-carboxylate ligated species **B**. Visible light excitation of **B** induces homolysis of the Ce—O bond of the η^1-carboxylate ligand to generate cerium(III)-containing species **C** and a carboxyl radical followed by decarboxylation, giving an alkyl radical. The alkyl radical reacts with **2** to form a hydrazyl radical that is rebound to the cerium(III) center for oxidation to cerium(IV) to afford (hydrazido)cerium(IV) species **D**. Abstraction of a proton by the (hydrazido)cerium(IV) moiety yields the final product **3** and carboxylic acid-free cluster **E**. Finally, carboxylic acid **1** coordinates to the cerium(IV) center to regenerate **A** and close the catalytic cycle. The role of manganese salts is to promote the re-oxidation step to form **D**, where incorporation of the manganese(II) species into the cluster increased

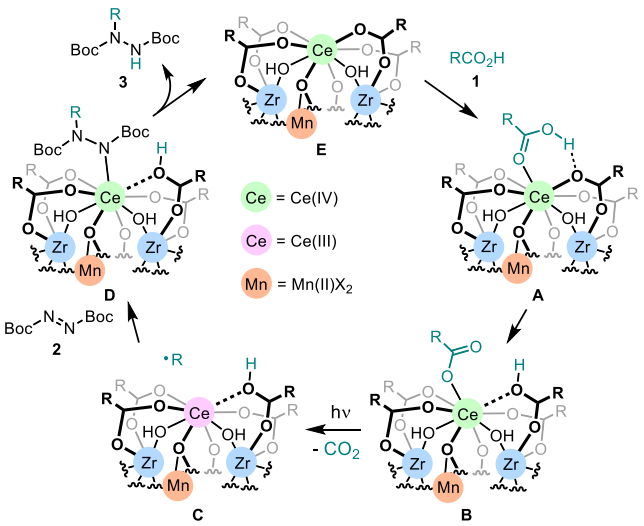

Scheme 1. Plausible mechanism for decarboxylative hydrazination catalyzed by **4a** and manganese salt.

Table 2: Decarboxylative hydrazination of **1c** with a phenol group.[a)]

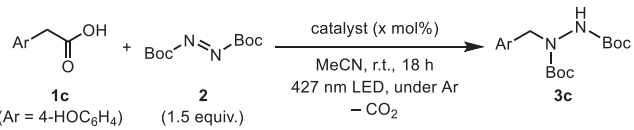

1c (Ar = 4-HOC$_6$H$_4$) + **2** (1.5 equiv.) → **3c**

Entry	Catalyst (x mol%)	Yield [%][b)]
1	**4a** (1.0), $Mn(OAc)_3{\cdot}2H_2O$ (2.0)	71 (65)[c)]
2	**4a** (1.0)	40
3	**4c** (1.0), $Mn(OAc)_3{\cdot}2H_2O$ (2.0)	n.d.
4	$Ce(O^tBu)_4$ (1.0), $Zr(O^tBu)_4$ (5.0) $Mn(OAc)_3{\cdot}2H_2O$ (2.0)	n.d.

n.d., not detected. [a)] Reaction conditions: **1c** (0.200 mmol), **2** (0.300 mmol), catalyst (x mol%), MeCN (3.0 mL), under Ar. Irradiated with 427 nm LED (distance between the light source and the test tube, 5 cm). [b)] Determined by ^{1}H NMR using 1,3,5-trimethoxybenzene as an internal standard. [c)] Isolated yield.

electron density of the cluster for accelerating the oxidation of the cerium(III) center to form (hydrazido)cerium(IV).

Substrate Scope for Decarboxylative Hydrazination

We applied $CeZr_5$ cluster **4a** as a catalyst for the hydrazination of 4-hydroxyphenylacetic acid (**1c**) containing a phenol group using a catalytic amount of $Mn(OAc)_3{\cdot}2H_2O$ in MeCN. This reaction, conducted under 427 nm LED irradiation, yielded the desired product **3c** in 71% yield without degradation of the phenol group (Table 2, entry 1). Because of the poor solubility of **1c** in PhCl, MeCN was used for this reaction. In the absence of $Mn(OAc)_3{\cdot}2H_2O$, **3c** was obtained in a moderate yield (entry 2). Notably, the following two catalysts, Ce_6 cluster **4c** and $Ce(O^tBu)_4/Zr(O^tBu)_4/Mn(OAc)_3{\cdot}2H_2O$ combination, showed no catalytic activity for decarboxylative hydrazination of **1c**, clearly indicating that the phenol group

Table 3: Substrate scope of carboxylic acids with OH, SH, and electron-rich arene ring.[a)]

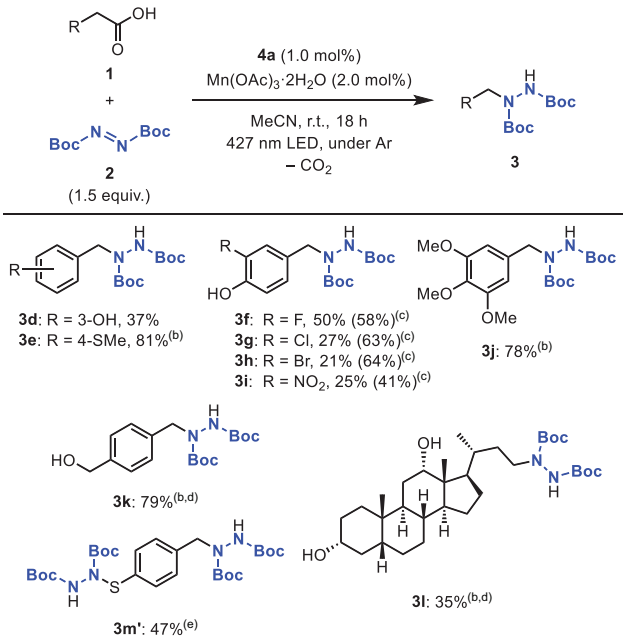

Isolated yields. [a)] Reaction conditions: **1** (0.200 mmol), **2** (0.300 mmol), **4a** (1.0 mol%), $Mn(OAc)_3{\cdot}2H_2O$ (2.0 mol%), MeCN (3.0 mL), under Ar. Irradiated with 427 nm LED (distance between the light source and the test tube, 5 cm). [b)] Three metal salts, $Ce(O^tBu)_4$ (1.0 mol%), $Zr(O^tBu)_4$ (5.0 mol%), and $Mn(OAc)_3{\cdot}2H_2O$ (2.0 mol%), were used as the catalyst under 390 nm LED light irradiation. [c)] **4a** (2.0 mol%) and $Mn(OAc)_3{\cdot}2H_2O$ (4.0 mol%) were used. [d)] EtOH, 42 h. [e)] Based on **2**.

served as a catalyst poison for cerium(IV) without the surrounding $Zr_5O_4(OH)_4$.

We screened various carboxylic acids with oxidizable functional groups, and the results are summarized in Table 3. The reactivity of 3-hydroxyphenylacetic acid (**1d**) was low compared with that of the 4-hydroxyphenyl derivative **1c**, giving the hydrazination product **3d** in 37% yield. This tendency of **1c** and **1d** was opposite that of the decarboxylative alkylation by an iron catalyst, in which the formation of **1c**-derived quinone methide slowed down the overall reaction rate:[58] In this hydrazination reaction, the electron-donating character of the 4-OH group affected the product yield. When 4-thiomethoxyphenylacetic acid (**1e**) was used, both **4a**/$Mn(OAc)_3{\cdot}2H_2O$ and the $Ce(O^tBu)_4/Zr(O^tBu)_4/Mn(OAc)_3{\cdot}2H_2O$ catalyst system were applicable to afford **3e** in high yields. 4-Hydroxyphenylacetic acids **1f–i**, bearing an electron-withdrawing substituent at the 3-position, were effectively converted into the corresponding hydrazination products **3f–i** in moderate yields using double amounts of **4a**/$Mn(OAc)_3{\cdot}2H_2O$ as a catalyst (2 mol% and 4 mol%, respectively). As observed in Table 2, utilization of cerium-incorporated cluster **4a** was key; otherwise, the yields of **3f–i** were less than 10% when combining the three metal salts, indicating that the phenol moiety was intact toward the cerium(IV) species in the $CeZr_5$ cluster core. 4-Hydroxyphenylacetic acids with electron-donating substituents such as methyl, methoxy, and hydroxy groups

Table 4: Substrate scope of carboxylic acids without phenol and thiol groups for decarboxylative hydrazination.[a)]

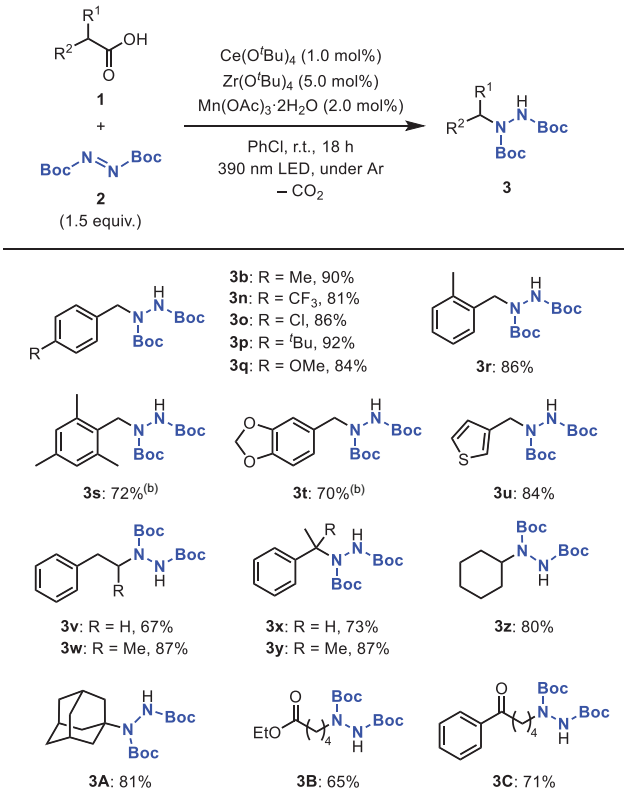

Isolated yields. [a)] Reaction conditions: **1** (0.200 mmol), **2** (0.300 mmol), Ce(O^{t}Bu)$_4$ (1.0 mol%), Zr(O^{t}Bu)$_4$ (5.0 mol%), Mn(OAc)$_3$·2H$_2$O (2.0 mol%), PhCl (3.0 mL), under Ar. Irradiated with 390 nm LED (distance between the light source and the test tube, 5 cm). [b)] MeCN.

Table 5: Optimization of reaction conditions for decarboxylative oxygenation of **1a**.[a)]

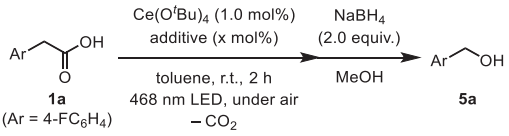

Entry	Additive (x mol%)	Yield [%][b)]
1	Zr(O^{t}Bu)$_4$ (5.0)	96
2	Zr(O^{t}Bu)$_4$ (5.0), Mn(OAc)$_3$·2H$_2$O (2.0)	77
3	Zr(O^{t}Bu)$_4$ (1.0)	46
4	Zr(O^{t}Bu)$_4$ (10)	83
5	Zr(acac)$_4$ (5.0)	85
6	–	10
7[c)]	Zr(O^{t}Bu)$_4$ (5.0)	n.d.
8	Hf(O^{t}Bu)$_4$ (5.0)	94
9	Ti(O^{t}Bu)$_4$ (5.0)	36
10	Nb(OEt)$_5$ (5.0)	13
11	Ta(OMe) (5.0)	21
12[d)]	Zr(O^{t}Bu)$_4$ (2.5)	93
13[d),e)]	Zr(O^{t}Bu)$_4$ (2.5)	93 (85)[f)]

n.d., not detected. [a)] Reaction conditions: **1a** (0.200 mmol), Ce(O^{t}Bu)$_4$ (1.0 mol%), additive (x mol%), toluene (3.0 mL), NaBH$_4$ (2.0 equiv.), MeOH (1.0 mL), under air. Irradiated with 468 nm LED (distance between the light source and the test tube, 5 cm). [b)] Determined by ^{1}H NMR using 1,3,5-trimethoxybenzene as an internal standard. [c)] Without Ce(O^{t}Bu)$_4$. [d)] **1a** (0.400 mmol), Ce(O^{t}Bu)$_4$ (0.5 mol%), 4 h. [e)] PhCl. [f)] Isolated yield.

were not applicable even when using **4a**, due to the susceptibility of the phenol moiety to oxidation (Table S11), whereas arylcarboxylic acid **1j** having three methoxy groups was converted to **3j** in a good yield, indicating that an electron-rich phenoxy ring was easily degraded under the catalytic conditions. A hydroxymethyl group in **1k** was tolerant to afford the hydrazinated product **3k** in a good yield by using ethanol as a solvent to dissolve **1k**. Naturally occurring carboxylic acid **1l** having two hydroxy groups was converted to **3l** without oxidation of the secondary alcohol groups. When 4-mercaptophenylacetic acid (**1m**) was used, C–N and S–N bond-forming product **3m'** was obtained in 47% yield based on **2** by using **4a** and Mn(OAc)$_3$·2H$_2$O, in which the thiophenol moiety reacts with azodicarboxylate to give the corresponding S–N bond-forming product under mild reaction conditions.

We further evaluated the applicability of various carboxylic acids without phenol and thiol groups using the three metal salt combinations, as shown in Table 4, under purple LED light (390 nm) irradiation to achieve better yields with a wide variety of the substrates (Table S7). 4-Substituted arylacetic acids **1b** and **1n–q** having both electron-donating and -withdrawing substituents were all applicable to give the corresponding decarboxylative hydrazinated products **3b** and **3n–q** in excellent yields. Sterically encumbered 2-methylphenylacetic acid (**1r**) and 2,4,6-trimethylphenylacetic acid (**1s**) afforded the C–N bond-forming products **3r** and **3s** in high yields without interruption by steric congestion at the *ortho*-positions. Carboxylic acids with an electron-rich piperonyl group and thienyl ring were also applicable to give **3t** and **3u**. Not only the primary aliphatic carboxylic acid **1v** but also secondary and tertiary aliphatic carboxylic acids **1w–A** were converted to the corresponding hydrazines in 67%–87% yields, respectively, without any suppression by the bulky substituents at the α-position of the carboxyl group. Ester and phenacyl functionalities at the terminal positions of aliphatic carboxylic acids **1B** and **1C** were all applicable under the reaction conditions, and the yields were comparable to the non-functionalized **1v**.

Decarboxylative Oxygenation by Ce-Zr Combined Catalysts

Mixed-metal CeZr$_5$ clusters were further applicable to the decarboxylative oxygenation reaction, as summarized in Table 5. A mixture of Ce(O^{t}Bu)$_4$ (1.0 mol%) and Zr(O^{t}Bu)$_4$ (5.0 mol%) in toluene showed excellent catalytic activity for successive decarboxylation and oxygenation to afford 4-fluorobenzyl alcohol (**5a**) in 96% yield after work-up with NaBH$_4$ in MeOH (entry 1), whereas no improvement of the product yield was observed upon the addition of Mn(OAc)$_3$·2H$_2$O (entry 2). Ce(O^{t}Bu)$_4$ (1.0 mol%) with lower or higher amounts of Zr(O^{t}Bu)$_4$ (1.0 mol% or 10 mol%)

decreased the yield of **5a** (entries 3 and 4; further details of the two metal ratios are provided in Table S16 in Supporting Information). $Zr(acac)_4$ also served as a good additive for this catalytic reaction, giving **5a** in 85% yield (entry 5), whereas other Zr(IV) complexes, such as $ZrO(NO_3)_2$, $Zr(OH)_4$, $ZrCl_4$, and metal oxide powders of ZrO_2 or CeO_2-ZrO_2, resulted in poor catalytic activity (Table S19). The catalytic activity of $Ce(O^tBu)_4$ (1.0 mol%) without Zr complexes under the identical reaction conditions was low, giving **5a** in 10% yield (entry 6), while no catalytic activity was observed for $Zr(O^tBu)_4$ or $Zr(acac)_4$ without $Ce(O^tBu)_4$ (entry 7 and Table S18, entry 8). The effects of other early transition metal alkoxides were further screened while maintaining a 1:5 ratio of cerium and the additive metal. As expected from the results in Table 1, the addition of $Hf(O^tBu)_4$ (5 mol%) enhanced the catalytic activity for this decarboxylative oxygenation to afford **5a** in 94% yield (entry 8), whereas $Ti(O^tBu)_4$ was less effective for this transformation (entry 9). The effect of group 5 metal alkoxides such as $Nb(OEt)_5$ and $Ta(OMe)_5$ was very small compared with group 4 metal alkoxides (entries 10 and 11), probably due to the difficulty in forming their heterobimetallic clusters. A half amount of $Ce(O^tBu)_4$ (0.5 mol%) and $Zr(O^tBu)_4$ (2.5 mol%) led to the formation of **5a** in 93% yield when the reaction time was extended to 4 h (entry 12), though a small amount of benzyl alcohol was detected as a contaminant due to the benzylic C–H oxidation of toluene,[93,94] the reaction solvent, during the extended reaction time. Chlorobenzene was found to be the optimal solvent to suppress the solvent oxidation, providing **5a** in 93% yield (entry 13, Table S20 for the solvent screening in Supporting Information).

We applied the optimized reaction conditions for this decarboxylative oxygenation to various carboxylic acids, as shown in Table 6. Treatment of arylacetic acids **1b** and **1n–q** afforded the corresponding alcohols **5b** and **5n–q** in moderate to high yields; among **1b** and **1n–q**, decarboxylation of **1q** with an electron-donating methoxy group resulted in a lower yield of **5q**, which was different from the result for the hydrazination reaction (vide infra). *Ortho*-methyl-substituted arylacetic acids were applicable, giving the C–O bond-forming products **5r** and **5s** in high yields, although a piperonyl group in **1t** suppressed the reaction to afford **5t** in a low yield. Lower yields using the electron-rich carboxylic acids **1q** and **1t** were ascribed to oxidative degradation in the presence of an external oxidant, dioxygen, which differs from the above-mentioned decarboxylative hydrazination reaction. Thienylacetic acid **1 u** exhibited moderate reactivity to give the corresponding alcohol **5u**. When 3-phenylpropanoic acid (**1v**) was used, 2-phenylethanol (**5v**) was obtained in only 25% yield, and extending the reaction time led to the formation of a one-carbon shortened alcohol, benzyl alcohol (**5v′**), as the byproduct (18 h, **5v**/**5v′** = 50%/12%). Small contamination of **5v′** was also observed from 2-methyl-3-phenylpropanoic acid (**1w**). In contrast, selective decarboxylative oxygenation of secondary and tertiary phenylacetic acids **1x** and **1y** afforded the corresponding alcohols **5x** and **5y** without any side products. Cholesterol **1l** was converted to **5l** without oxidation of the secondary alcohol moieties in the presence of dioxygen.

Table 6: Substrate scope of carboxylic acids with OH, SH, and electron-rich arene ring.[a)]

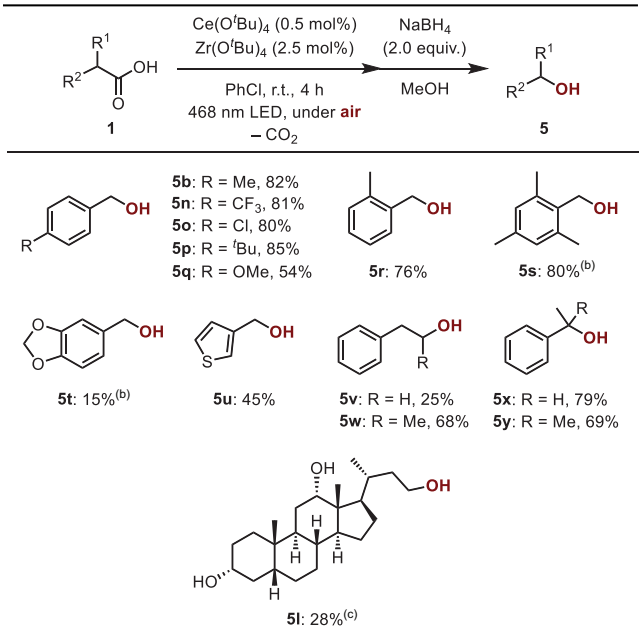

Isolated yields. [a)] Reaction conditions: **1** (0.400 mmol), $Ce(O^tBu)_4$ (0.5 mol%), $Zr(O^tBu)_4$ (2.5 mol%), PhCl (3.0 mL), $NaBH_4$ (2.0 equiv.), MeOH (1.0 mL), under air. Irradiated with 468 nm LED (distance between the light source and the test tube, 5 cm). [b)] MeCN, 8 h. [c)] EtOH, 18 h.

Hammett analysis of this decarboxylative oxygenation for *p*-substituted arylacetic acids using **4a** as the catalyst was carried out to clarify the electronic effect of the substrates on the reaction progress (Figure S17).[95,96] Compared with 4-trifluoromethyl-substituted arylcarboxylic acid **1n**, substrates **1a,b,o** afforded the alcohols in higher yields in a short reaction time. In sharp contrast, when using *p*-methoxy-substituted one **1q** deviated from the tendency; in fact, the final yield of **5q** was lower than that of **5n**, as shown in Table 6. Monitoring the reaction progress of **1q** using **4a** as the catalyst revealed the formation of corresponding oxygenated products (4-methoxybenzyl alcohol (**5q**), 4-methoxybenzaldehyde (**6q**), and 4-methoxybenzyl hydroperoxide (**7q**)) in an 80% total yield over a longer reaction time (9 h), but no further increase in the yield was observed after 9 hours, which is in contrast to the slow but continuous increase in the yield when using **1n** (Figure S18). Phenol-substituted carboxylic acid **1c** was not applicable for this decarboxylative alcohol synthesis, indicating that an external oxidant affected the functional group tolerance toward the electron-rich substrate.

In summary, we demonstrated that in situ generated multi-element clusters containing cerium(IV) exhibited excellent catalytic activity for the decarboxylative functionalization of aliphatic carboxylic acids. Single cerium(IV)-containing hexanuclear mixed-metal clusters **4a** and **4b** were isolated and structurally characterized via single metal-to-metal substitution of the hexanuclear zirconium and hafnium clusters, and **4a** and **4b** were photo-reduced with the generation of one equivalent of the alkyl radical per one cluster molecule.

Furthermore, the catalytic activity of the heterometallic clusters for decarboxylative hydrazination was significantly improved upon addition of the third metal ion to the reaction mixture; the remarkable enhancement of the catalytic activity was due to the interaction of the third element with the mixed-metal $CeZr_5O_4(OH)_4$ core to assist re-oxidation of the photo-reduced cerium(III)-containing clusters. Further studies to develop new catalytic transformations using heterometallic clusters by post-modification of the original homometallic clusters are ongoing in our laboratory.

Acknowledgements

S.T. thanks the financial support by the JSPS Research Fellowships for Young Scientists. The authors appreciate fruitful discussion with Dr. Satoru Shirase and Dr. Tomomi Kawakami in the early stage of this research. This work was supported by JSPS KAKENHI Grant Nos. JP20H02742 and JP24K01486 (Grant-in-Aid for Scientific Research(B)), JP21K01486 (Grant-in-Aid for Challenging Research (Exploratory)), JP24H01080 (Digitalization-driven Transformative Organic Synthesis), JP24H01853 (Green Catalysis Science for Renovating Transformation of Carbon-Based Resources) to H.T., and JP23H04906 (Green Catalysis Science for Renovating Transformation of Carbon-Based Resources) to M.F. This work was supported in part by Grant for Basic Science Research Projects from The Sumitomo Foundation (H.T.).

Conflict of Interests

The authors declare no conflict of interest.

Data Availability Statement

The data that support the findings of this study are available in the Supporting Information of this article.

Keywords: Carboxylic acid · Cerium · Manganese · Zirconium

[1] M. H. Shaw, J. Twilton, D. W. C. MacMillan, *J. Org. Chem.* **2016**, *81*, 6898–6926.
[2] N. A. Romero, D. A. Nicewicz, *Chem. Rev.* **2016**, *116*, 10075–10166.
[3] J. Twilton, C. Le, P. Zhang, M. H. Shaw, R. W. Evans, D. W. C. MacMillan, *Nat. Rev. Chem.* **2017**, *1*, 1–19.
[4] K. P. S. Cheung, S. Sarkar, V. Gevorgyan, *Chem. Rev.* **2022**, *122*, 1543–1625.
[5] A. Y. Chan, I. B. Perry, N. B. Bissonnette, B. F. Buksh, G. A. Edwards, L. I. Frye, O. L. Garry, M. N. Lavagnino, B. X. Li, Y. Liang, E. Mao, A. Millet, J. V. Oakley, N. L. Reed, H. A. Sakai, C. P. Seath, D. W. C. MacMillan, *Chem. Rev.* **2022**, *122*, 1485–1542.
[6] S. Gavelle, M. Innocent, T. Aubineau, A. Guérinot, *Adv. Synth. Catal.* **2022**, *364*, 4189–4230.
[7] L. Li, Y. Yao, N. Fu, *Eur. J. Org. Chem.* **2023**, *26*, e202300166.
[8] J. D. Tibbetts, H. E. Askey, Q. Cao, J. D. Grayson, S. L. Hobson, G. D. Johnson, J. C. Turner-Dore, A. J. Cresswell, *Synthesis* **2023**, *55*, 3239–3250.
[9] S. Mondal, S. Mandal, S. Mondal, S. P. Midya, P. Ghosh, *Chem. Commun.* **2024**, *60*, 9645–9658.
[10] J.-L. Tu, Z. Shen, B. Huang, *Adv. Synth. Catal.* **2024**, *366*, 1–12.
[11] C.-Q. Deng, J. Deng, *Green Chem.* **2025**, *27*, 275–292.
[12] H. Tsurugi, K. Mashima, *J. Am. Chem. Soc.* **2021**, *143*, 7879–7890.
[13] Y. Abderrazak, A. Bhattacharyya, O. Reiser, *Angew. Chem. Int. Ed.* **2021**, *60*, 21100–21115.
[14] F. Juliá, *ChemCatChem* **2022**, *14*, e202200916.
[15] L. H. M. de Groot, A. Ilic, J. Schwarz, K. Wärnmark, *J. Am. Chem. Soc.* **2023**, *145*, 9369–9388.
[16] A. Reichle, O. Reiser, *Chem. Sci.* **2023**, *14*, 4449–4462.
[17] R. A. Sheldon, J. K. Kochi, *J. Am. Chem. Soc.* **1968**, *90*, 6688–6698.
[18] V. R. Yatham, P. Bellotti, B. König, *Chem. Commun.* **2019**, *55*, 3489–3492.
[19] K. Wadekar, S. Aswale, V. R. Yatham, *Org. Biomol. Chem.* **2020**, *18*, 983–987.
[20] S. Shirase, S. Tamaki, K. Shinohara, K. Hirosawa, H. Tsurugi, T. Satoh, K. Mashima, *J. Am. Chem. Soc.* **2020**, *142*, 5668–5675.
[21] X.-L. Lai, X.-M. Shu, J. Song, H.-C. Xu, *Angew. Chem. Int. Ed.* **2020**, *59*, 10626–10632.
[22] A. R. Tripathy, G. S. Yedase, V. R. Yatham, *RSC Adv.* **2021**, *11*, 25207–25210.
[23] S. Singh, N. Dagar, S. R. Roy, *Chem. Commun.* **2022**, *58*, 3831–3834.
[24] H.-C. Li, G.-N. Li, K. Sun, X.-L. Chen, M.-X. Jiang, L.-B. Qu, B. Yu, *Org. Lett.* **2022**, *24*, 2431–2435.
[25] N. Dagar, S. Singh, S. Raha Roy, *J. Org. Chem.* **2022**, *87*, 8970–8982.
[26] Y. Wang, L. Li, N. Fu, *ACS Catal.* **2022**, *12*, 10661–10667.
[27] X.-L. Lai, M. Chen, Y. Wang, J. Song, H.-C. Xu, *J. Am. Chem. Soc.* **2022**, *144*, 20201–20206.
[28] T. Kawakami, S. Tamaki, S. Shirase, H. Tsurugi, K. Mashima, *Inorg. Chem.* **2022**, *61*, 20461–20471.
[29] Y. Xu, P. Huang, Y. Jiang, C. Lv, P. Li, J. Wang, B. Sun, C. Jin, *Green Chem.* **2023**, *25*, 8741–8747.
[30] J. Lu, Y. Yao, L. Li, N. Fu, *J. Am. Chem. Soc.* **2023**, *145*, 26774–26782.
[31] R. Guan, G. Chen, E. L. Bennett, Z. Huang, J. Xiao, *Org. Lett.* **2023**, *25*, 2482–2486.
[32] M. Wang, D. Wang, K. Xu, C. Zeng, *Catal. Sci. Technol.* **2024**, *14*, 1037–1042.
[33] C. A. Parker, *Proc. R. Soc. Lond. A* **1953**, *220*, 104–116.
[34] C. G. Hatchard, C. A. Parker, *Proc. R. Soc. Lond. A* **1956**, *235*, 518–536.
[35] A. Sugimori, T. Yamada, *Chem. Lett.* **1986**, *15*, 409–412.
[36] A. Sugimori, T. Yamada, *Bull. Chem. Soc. Jpn.* **1986**, *59*, 3911–3915.
[37] Z. Li, X. Wang, S. Xia, J. Jin, *Org. Lett.* **2019**, *21*, 4259–4265.
[38] G. Feng, X. Wang, J. Jin, *Eur. J. Org. Chem. 2019*, 6728–6732.
[39] S. Xia, K. Hu, C. Lei, J. Jin, *Org. Lett.* **2020**, *22*, 1385–1389.
[40] K. Niu, P. Zhou, L. Ding, Y. Hao, Y. Liu, H. Song, Q. Wang, *ACS Sustainable Chem. Eng.* **2021**, *9*, 16820–16828.
[41] Y. Zhang, J. Qian, M. Wang, Y. Huang, P. Hu, *Org. Lett.* **2022**, *24*, 5972–5976.
[42] J.-L. Tu, H. Gao, M. Luo, L. Zhao, C. Yang, L. Guo, W. Xia, *Green Chem.* **2022**, *24*, 5553–5558.
[43] H. Kang, S. An, S. Lee, *Org. Chem. Front.* **2023**, *10*, 5151–5157.
[44] M. Innocent, G. Lalande, F. Cam, T. Aubineau, A. Guérinot, *Eur. J. Org. Chem.* **2023**, *26*, e202300892.

[45] Y.-C. Lu, J. G. West, *Angew. Chem. Int. Ed.* **2023**, *62*, e202213055.
[46] K.-J. Bian, Y.-C. Lu, D. Nemoto, S.-C. Kao, X. Chen, J. G. West, *Nat. Chem.* **2023**, *15*, 1683–1692.
[47] A.-M. Hu, J.-L. Tu, M. Luo, C. Yang, L. Guo, W. Xia, *Org. Chem. Front.* **2023**, *10*, 4764–4773.
[48] N. Xiong, Y. Li, R. Zeng, *ACS Catal.* **2023**, *13*, 1678–1685.
[49] S. Fernández-García, V. O. Chantzakou, F. Juliá-Hernández, *Angew. Chem. Int. Ed.* **2024**, *63*, e202311984.
[50] Y. Zhu, H. Gao, J.-L. Tu, C. Yang, L. Guo, Y. Zhao, W. Xia, *Org. Chem. Front.* **2024**, *11*, 1729–1735.
[51] X.-K. Qi, L.-J. Yao, M.-J. Zheng, L. Zhao, C. Yang, L. Guo, W. Xia, *ACS Catal.* **2024**, *14*, 1300–1310.
[52] J. Qian, Y. Zhang, W. Zhao, P. Hu, *Chem. Commun.* **2024**, *60*, 2764–2767.
[53] A. Fall, M. Magdei, M. Savchuk, S. Oudeyer, H. Beucher, J.-F. Brière, *Chem. Commun.* **2024**, *60*, 6316–6319.
[54] L. M. Denkler, M. Aladahalli Shekar, T. S. J. Ngan, L. Wylie, D. Abdullin, M. Engeser, G. Schnakenburg, T. Hett, F. H. Pilz, B. Kirchner, O. Schiemann, P. Kielb, A. Bunescu, *Angew. Chem. Int. Ed.* **2024**, *63*, e202403292.
[55] M. Innocent, C. Tanguy, S. Gavelle, T. Aubineau, A. Guérinot, *Chem. - Eur. J.* **2024**, *30*, e202401252.
[56] R. Nsouli, S. Nayak, V. Balakrishnan, J.-Y. Lin, B. K. Chi, H. G. Ford, A. V. Tran, I. A. Guzei, J. Bacsa, N. R. Armada, F. Zenov, D. J. Weix, L. K. G. Ackerman-Biegasiewicz, *J. Am. Chem. Soc.* **2024**, *146*, 29551–29559.
[57] M. S. Crocker, J.-Y. Lin, R. Nsouli, N. D. McLaughlin, D. G. Musaev, A. Mehranfar, E. R. Lopez, L. K. G. Ackerman-Biegasiewicz, *Chem Catal* **2024**, *4*, 101131.
[58] S. Tamaki, T. Kusamoto, H. Tsurugi, *Chem. - Eur. J.* **2024**, *30*, e202402705.
[59] W. Su, P. Xu, T. Ritter, *Angew. Chem. Int. Ed.* **2021**, *60*, 24012–24017.
[60] P. Xu, P. López-Rojas, T. Ritter, *J. Am. Chem. Soc.* **2021**, *143*, 5349–5354.
[61] P. Xu, W. Su, T. Ritter, *Chem. Sci.* **2022**, *13*, 13611–13616.
[62] A. Reichle, H. Sterzel, P. Kreitmeier, R. Fayad, F. N. Castellano, J. Rehbein, O. Reiser, *Chem. Commun.* **2022**, *58*, 4456–4459.
[63] Q. Y. Li, S. N. Gockel, G. A. Lutovsky, K. S. DeGlopper, N. J. Baldwin, M. W. Bundesmann, J. W. Tucker, S. W. Bagley, T. P. Yoon, *Nat. Chem.* **2022**, *14*, 94–99.
[64] N. W. Dow, P. S. Pedersen, T. Q. Chen, D. C. Blakemore, A.-M. Dechert-Schmitt, T. Knauber, D. W. C. MacMillan, *J. Am. Chem. Soc.* **2022**, *144*, 6163–6172.
[65] T. Q. Chen, P. S. Pedersen, N. W. Dow, R. Fayad, C. E. Hauke, M. C. Rosko, E. O. Danilov, D. C. Blakemore, A.-M. Dechert-Schmitt, T. Knauber, F. N. Castellano, D. W. C. MacMillan, *J. Am. Chem. Soc.* **2022**, *144*, 8296–8305.
[66] P. P. Sen, S. Raha Roy, *Organometallics* **2023**, *42*, 1658–1666.
[67] Y. Yuan, J. Yang, J. Zhang, *Chem. Sci.* **2023**, *14*, 705–710.
[68] P. S. Pedersen, D. C. Blakemore, G. M. Chinigo, T. Knauber, D. W. C. MacMillan, *J. Am. Chem. Soc.* **2023**, *145*, 21189–21196.
[69] Z. He, P. Dydio, *Angew. Chem. Int. Ed.* **2024**, *63*, e202410616.
[70] S. Tamaki, T. Kusamoto, H. Tsurugi, *ChemCatChem* **2025**, *17*, e202402106.
[71] C.-L. Ji, Y.-N. Lu, S. Xia, C. Zhu, C. Zhu, W. Li, J. Xie, *Angew. Chem. Int. Ed.* **2025**, *64*, e202423113.
[72] M. Lammert, C. Glißmann, N. Stock, *Dalton Trans.* **2017**, *46*, 2425–2429.
[73] K. A. Lomachenko, J. Jacobsen, A. L. Bugaev, C. Atzori, F. Bonino, S. Bordiga, N. Stock, C. Lamberti, *J. Am. Chem. Soc.* **2018**, *140*, 17379–17383.
[74] J. Jacobsen, H. Reinsch, N. Stock, *Inorg. Chem.* **2018**, *57*, 12820–12826.
[75] E. Geravand, F. Farzaneh, R. Gil-San-Millan, F. J. Carmona, J. A. R. Navarro, *Inorg. Chem.* **2020**, *59*, 16160–16167.
[76] C. Atzori, K. A. Lomachenko, J. Jacobsen, N. Stock, A. Damin, F. Bonino, S. Bordiga, *Dalton Trans.* **2020**, *49*, 5794–5797.
[77] M. Ronda-Lloret, I. Pellicer-Carreño, A. Grau-Atienza, R. Boada, S. Diaz-Moreno, J. Narciso-Romero, J. C. Serrano-Ruiz, A. Sepúlveda-Escribano, E. V. Ramos-Fernandez, *Adv. Funct. Mater.* **2021**, *31*, 2102582.
[78] A. Valverde-González, M. Pintado-Sierra, A. Rasero-Almansa, F. Sánchez, M. Iglesias, *Appl. Catal. A* **2021**, *623*, 118287.
[79] X. Zhang, X. Li, W. Gao, S. Luo, S. Su, R. Huang, M. Luo, *Sustainable Energy Fuels* **2021**, *5*, 4053–4059.
[80] A. Bhattacharyya, M. Gutiérrez, B. Cohen, H. Szalad, J. Albero, H. Garcia, A. Douhal, *ACS Appl. Mater. Interfaces* **2023**, *15*, 36434–36446.
[81] C. Yu, X. Zhang, C. Song, Y. Wang, J. Lin, Z. Guo, Y. Zhang, Z. Liu, C. Li, Y. Sun, C. Tang, Y. Huang, *Chem. Eng. J.* **2024**, *499*, 156088.
[82] See Supporting Information for transient absorption spectra of Ce_6, **4a**, and **4b**. Longer lifetime of **4a** and **4b** compared with Ce_6 for the excited state indicates the enough lifetime for **4a** and **4b** to release the carboxylate radicals via homolysis of the metal-ligand covalent bond. See Figure S29 in SI.
[83] I. L. Malaestean, M. Speldrich, A. Ellern, S. G. Baca, P. Kögerler, *Dalton Trans.* **2011**, *40*, 331–333.
[84] V. Mereacre, A. M. Ako, M. N. Akhtar, A. Lindemann, C. E. Anson, A. K. Powell, *Helv. Chim. Acta* **2009**, *92*, 2507–2524.
[85] I. L. Malaestean, M. K. Alıcı, C. Besson, A. Ellern, P. Kögerler, *CrystEngComm* **2014**, *16*, 43–46.
[86] S. Schmitz, N. V. Izarova, J. van Leusen, K. Kleemann, K. Y. Monakhov, P. Kögerler, *Inorg. Chem.* **2021**, *60*, 11599–11608.
[87] M. Seiß, J. Lorenz, S. Schmitz, M. Moors, M. Börner, K. Y. Monakhov, *Dalton Trans.* **2024**, *53*, 8454–8462.
[88] G. Maayan, G. Christou, *Inorg. Chem.* **2011**, *50*, 7015–7021.
[89] C. Papatriantafyllopoulou, K. A. Abboud, G. Christou, *Polyhedron* **2013**, *52*, 196–206.
[90] C. Lampropoulos, A. E. Thuijs, K. J. Mitchell, K. A. Abboud, G. Christou, *Inorg. Chem.* **2014**, *53*, 6805–6816.
[91] S. Das Gupta, R. L. Stewart, D.-T. Chen, K. A. Abboud, H.-P. Cheng, S. Hill, G. Christou, *Inorg. Chem.* **2020**, *59*, 8716–8726.
[92] S. Das Gupta, A. E. Thuijs, E. G. Fisher, K. A. Abboud, G. Christou, *Inorg. Chem.* **2022**, *61*, 6392–6402.
[93] S. Mukherjee, B. Maji, A. Tlahuext-Aca, F. Glorius, *J. Am. Chem. Soc.* **2016**, *138*, 16200–16203.
[94] M. Hirose, H. Sakaguchi, R. Hashimoto, T. Furutani, M. Yamawaki, H. Suzuki, Y. Yoshimi, *Chem. - Eur. J.* **2024**, *30*, e202402285.
[95] H. M. Yau, A. K. Croft, J. B. Harper, *Chem. Commun.* **2012**, *48*, 8937.
[96] C. Hansch, A. Leo, R. W. Taft, *Chem. Rev.* **1991**, *91*, 165–195.

Manuscript received: March 11, 2025
Revised manuscript received: May 22, 2025
Accepted manuscript online: June 06, 2025
Version of record online: June 18, 2025